Published in final edited form as:
Nature. 2014 January 23; 505(7484): 564–568. doi:10.1038/nature12819.

Glutamine methylation in Histone H2A is an RNA Polymerase I dedicated modification

Peter Tessarz[1], **Helena Santos-Rosa**[1], **Sam C. Robson**[1], **Kathrine B. Sylvestersen**[2], **Christopher J Nelson**[1,3], **Michael L. Nielsen**[2], and **Tony Kouzarides**[1,*]

[1]Gurdon Institute and Department of Pathology, Tennis Court Road, Cambridge CB2 1QN, UK

[2]Department of Proteomics, The Novo Nordisk Foundation Center for Protein Research, Faculty of Health Sciences, University of Copenhagen, Blegdamsvej 3B, DK-2200 Copenhagen, Denmark

Abstract

Nucleosomes are decorated with numerous post-translational modifications capable of influencing many DNA processes[1]. Here, we describe a new class of histone modification, methylation of glutamine, occurring on yeast histone H2A at position 105 (Q105) and human H2A at Q104. We identify Nop1 as the methyltransferase in yeast and demonstrate that Fibrillarin is the ortholog enzyme in human cells. Glutamine methylation of H2A is restricted to the nucleolus. Global analysis in yeast, using an H2AQ105me specific antibody, show that this modification is exclusively enriched over the 35S rDNA transcriptional unit. We show that the Q105 residue is part of the binding site for the histone chaperone FACT (Facilitator of Transcription) complex[2]. Methylation of Q105 or its substitution to alanine disrupts binding to FACT *in vitro*. A yeast strain mutated at Q105 exhibits reduced histone incorporation and increased transcription at the rDNA locus. These features are phenocopied by mutations in FACT complex components. Together these data identify glutamine methylation of H2A as the first histone epigenetic mark dedicated to a specific RNA polymerase and define its function as a regulator of FACT interaction with nucleosomes.

Glutamine methylation occurs on translation termination factors and ribosomal proteins[3]. We investigated whether such a modification exists on histones by interrogating mass spectrometric (MS) datasets. We identified a single glutamine, human Q104 (yeast: Q105) in H2A as a site of methylation (Fig. 1a and Extended Data Fig. 1). The residue is located on the surface of the octamer (Extended Data Fig. 2) and is highly conserved in canonical H2A from yeast to human. However, in H2A.Z it is exchanged for a glycine or serine (Fig. 1b). We raised a modification specific antibody (Extended Data Fig. 3) that detects this modification in yeast and mammalian cells (Fig. 1c).

*Corresponding Author: Tony Kouzarides (t.kouzarides@gurdon.cam.ac.uk) .
[3]Present address: Dept. Biochemistry & Microbiology, University of Victoria, 3800 Finnerty Road, Victoria BC V8P 5C2, Canada

Author Contribution P.T. and H.S.-R. designed experiments, performed research, interpreted data and wrote the manuscript. K.B.S. and M.L.N. performed mass spectrometric analysis. C.J.N. supplied new reagents. T.K. designed experiments, interpreted data and wrote the manuscript.

T.K. is a founder of Abcam Ltd.

Author Information The data of the ChIP-Seq experiments were submitted to Array Express with the accession code E-MTAB-1447 (https://www.ebi.ac.uk/arrayexpress/experiments/E-MTAB-1447/).

Europe PMC Funders Author Manuscripts

To identify the methyltransferase responsible, we performed a candidate approach and screened 72 predicted non-essential yeast methyltransferases[4] by analysing knock-out lysates via western blotting with the modification specific antibody. However, we did not detect loss of signal in any lysate (not shown). We then used an unbiased biochemical approach and fractionated yeast cells as described in Figure 2a. Fractions were assayed on a 20-mer peptide spanning Q105, or the respective QA mutant, coupled to beads in the presence of [^{3}H]-S-Adenosyl-Methionine (SAM). Methyltransferase activity was assessed by scintillation counting (Fig. 2b) and the fraction containing activity towards H2AQ105 was subjected to MS analysis (Supplementary Table 4). All 178 non-essential proteins identified by MS were tested by knock-out analysis and western blotting, but none showed reduction of Q105 methylation (not shown). We then examined the essential proteins within the active fraction. We focused on Nop1, a known rRNA methyltransferase[5], since its essential co-factors, Nop56/58[6] and other members of an active RNA Polymerase I complex[7] were present within this active fraction. Furthermore, with the exception of Nop58, all above mentioned proteins are known to interact with H2A[8,9]. TAP-tag purification of the Nop1 complex purifies an enzymatic activity that methylates H2AQ105 (Fig. 2c). Next, recombinantly purified Nop1 was tested for its ability to modify recombinant H2A *in vitro*. Indeed, Nop1, in the presence of H2A and SAM, methylates H2AQ105 as detected by the H2AQ105me specific antibody (Figure 2d and Extended Data Fig. 4a). Additionally, MS analysis of this reaction identifies H2AQ105 methylation (Figure 2e and Extended Data Fig. 4b). To test the enzymatic activity of Nop1 *in vivo* we made use of two independently isolated thermosensitive mutants carrying the same amino acid changes, which are located within Nop1's SAM binding site[5]. Yeast harbouring these ts-alleles showed a 50% reduced Q105 methylation signal upon shift to restrictive temperature at a time at which cells are still proliferating (Fig. 2f and Extended Data Fig. 5a,b). These results identify Nop1 as the enzyme responsible for H2AQ105 methylation in yeast.

Nop1 has a single highly conserved homologue in human cells, called Fibrillarin[10] (Extended Data Fig.5c,d). To establish that Fibrillarin methylates Q104 methylation in human cells, it was knocked-down in MCF10A cells. Transfection of two independent siRNAs against Fibrillarin leads to robustly reduced levels of H2AQ104me (Fig. 2g and Extended Data Fig. 5e). At this time viability was only marginally affected, based on MTT proliferation assays (Extended Data Fig. S5f). Furthermore, immunofluorescence showed that Q104me and Fibrillarin were enriched in the nucleolus of MCF10A cells (Fig. 2h). However, siRNA induced knock-down of Fibrillarin completely abrogated detection of Q104me in the nucleolus. Importantly, we observed no morphological changes of the nucleus and nucleolus that have been reported to occur upon prolonged Fibrillarin knock-down[11], indicating that - in agreement with the MTT assay - the viability of the cells was not affected at the time of analysis.

The main function of the nucleolus is rDNA transcription and ribosome biogenesis[12]. To analyse the distribution of H2A glutamine methylation in chromatin, we performed chromatin immunoprecipitations coupled to deep DNA sequencing (ChIP-Seq). The rDNA locus consists of roughly 100 to 200 repeats in yeast and 200-400 copies in human cells[13] of which about half are active and almost devoid of nucleosomal structure and the other half are inactive and densely packed with nucleosomes[13,14]. In yeast up to ~80% of rDNA repeats can be deleted, in which case all the remaining repeats, ~20 copies, are active[15]. This strain still retains H2AQ105me (Extended Data Fig. 6). Remarkably, when the H2AQ105me antibody is used in ChIP-Seq analysis, the only site of enrichment within the entire yeast genome is over the 35S rDNA transcription units (Fig. 3 a,c). In addition, Nop1, the enzyme that mediates H2AQ105 methylation, colocalises with H2AQ105 methylation at the 35S rDNA locus (Fig. 3d). Together, these results indicate that in both human and yeast, methylation of H2A represents a modification restricted to the nucleolus. Given the

enrichment of glutamine methylation on the transcribed region of the rDNA cluster, we asked if RNA Polymerase I transcription was required for deposition of Q105 methylation. We used Actinomycin D at concentration known to inhibit RNA Polymerase I, but not RNA Polymerase II[16]. These conditions led to reduced Q104/5 methylation in mammalian/yeast cells, indicating that active RNA Pol I transcription is required for glutamine methylation to occur (Extended Data Fig. 7).

Histone methylation can act as a platform to recruit and regulate other chromatin-related factors[1] such as chromatin remodelling complexes. The region spanning Q105 within H2A has previously been described as a potential binding site for FACT[17,18], a protein complex consisting of Spt16/Pob3 and Nhp6a in yeast, which is required for efficient passage of RNA and DNA polymerases through chromatin by remodelling nucleosomes[2]. Residues within the region of H2A spanning Q105 show genetic interactions with FACT ts mutants[17,18], as does a Q105A mutant using a transcription based reporter system (Extended Data Fig. 8).

To probe the possibility that FACT physically interacts with H2A via the region spanning Q105, we took an unbiased approach (phage display) to identify regions within H2A/H2B interacting with Spt16 and Pob3. A randomised 12-mer peptide phage library was used to enrich for sequences binding to Spt16/Pob3. In line with the published genetic findings, the interaction screen identified a consensus sequence spanning H2AQ105 as the binding site for FACT (Extended Data Fig. 9a).

We next asked whether methylation of H2AQ105 could influence the binding to FACT. Figure 4a shows that binding of recombinant Spt16/Pob3 to a peptide spanning H2AQ105 is significantly decreased when Q105 is methylated or mutated to alanine. Pull-downs from HeLa nuclear extracts using the same peptides demonstrate that the endogenous human FACT complex is responsive to glutamine methylation on H2A (Extended Data Fig. 9b), suggesting that the disruption of FACT binding to this site is the mechanistic consequence of glutamine methylation.

We next sought to explore the consequence of H2AQ105 methylation on FACT function *in vivo*. To do this we took advantage of the fact that mutation of H2AQ105 to alanine phenocopies Q105 methylation in terms of effecting FACT binding (Fig 4a). To study a potential influence of Q105 methylation on rDNA transcription and its interplay with FACT, we turned to a well-established reporter-based system that allows sensitive monitoring of the transcriptional state of the rDNA locus, in which weak, but constitutively expressed *URA3* cassettes were integrated into the rDNA locus (S3 and S6; Fig. 4b)[19]. Figure 4b shows a significant drop in 5-FOA positive colonies in the Q105A mutant indicative of a higher transcription rate of the *URA3*. We then introduced the *spt16-11* allele – which leads to a 30-40% decrease of FACT protein levels[17] - into the same reporter strains. Figure 4d shows that at semi-permissive temperature we observe a drastic loss of colony numbers on 5-FOA plates, pointing to an increase in transcriptional activity in accordance with recently published findings[20]. These results show that reduced FACT activity indeed phenocopies the Q105A mutation. Thus, a mutation that disrupts the function of the chromatin remodeler FACT or a mutation that disrupts the binding of FACT to chromatin lead to transcriptional permissiveness at the rDNA locus. To directly monitor RNA Pol I transcription rates we performed run-on experiments in wild-type, FACT *ts* and Q105A strains. Figure 4d shows that rDNA transcription was increased using two different primer pairs confirming a more permissive chromatin at the rDNA locus, when FACT or Q105A are mutated.

One possible explanation for the increased rDNA transcription in the Q105A and FACT ts strains, is loss of nucleosomes over a transcribed region. FACT ts mutants have already been

described as possessing such a phenotype[21]. To investigate a possible histone deposition defect, we generated strains in which we placed myc-tagged versions of either wild-type H2A or the Q105A mutant under control of the Gal1-promoter in a wild-type or *spt16-11* yeast background. Induction of the myc-tagged histones was identical as judged by total steady-state levels on western blots (Extended Data Fig. 10a). The wild-type H2A was very efficiently deposited into chromatin as monitored by ChIP (Fig. 4e). However, the *spt16-11* and the Q105A mutant had a profound defect in incorporation into chromatin (Fig. 4e). These findings suggest that methylation of H2AQ105, as phenocopied by the H2AQ105A mutation and a FACT ts mutant, result in the transcriptional stimulation of the *URA3* reporters due to reduced nucleosomal occupancy within the rDNA repeat.

Finally, we set out to directly test, whether increase in Q105 methylation on the rDNA locus would decrease FACT occupancy. Indeed, over-expression of Nop1 leads to increased Q105me and is accompanied by a decrease of FACT occupancy, in line with the hypothesis that Q105 methylation is regulating FACT availability on chromatin (Fig. 4f).

The findings presented here identify a new histone modification pathway operational exclusively in the nucleolus. It involves methylation of H2AQ105 by Nop1 in yeast, and methylation of H2AQ104 by Fibrillarin in human cells, resulting in the weakening of interactions between H2A and FACT. The FACT complex interacts with all three RNA polymerases[22,23] and facilitates transcription in two steps by (a) binding and disrupting nucleosomes in the path of the polymerase[22,24,25] and (b) by augmenting the re-deposition of nucleosomes in the wake of transcribing polymerase[24,26]. Glutamine methylation of H2A may affect either of these functions by disrupting binding to FACT. The observation that an H2AQ105A mutant is incorporated to a lower extent would favour a model in which re-deposition is decreased. Such a model is also in agreement with earlier observations that rDNA has a low nucleosome occupancy[13] in contrast to most other regions of the genome. Indeed, recent reports suggest that H2A in particular appears to be depleted from this region[27] and that FACT might play a role in this pathway[20]. The net result of a glutamine modified chromatin state is that RNA Pol I transits less impeded by nucleosomes. It is worth noting however that glutamine methylation of H2A is present within the rDNA locus, even though deposition is affected. The residual loading of modified H2A might be due to the presence of other histone chaperones such as Nap1 that are insensitive to glutamine methylation on H2A (Extended Data Fig. 10b).

RNA Pol I associates with the Nop1 enzyme and may carry it along during transcription elongation. It is currently unclear how glutamine methylation is initiated or reversed, but it might be linked to the re-activation of the rDNA locus that has been described to occur after DNA replication in an RNA PolI dependent manner[27]. Another possibility is that the enzyme itself is the key node of regulation. Nop1/Fibrillarin is highly modified[28,29], so a signalling pathway leading to the glutamine methyltransferase could be the triggering event.

Glutamine methylation of H2A represents the first histone modification that is dedicated to only one of the three RNA polymerases. The selectivity for Pol I and its compartmentalisation within the nucleolus might be necessary to generate a chromatin state capable of dealing with the high demands for transcription of ribosomal components. Indeed, glutamine methylation as a whole appears to be a modification that is dedicated to ribosomal biosynthesis: Nop1 has the ability to also methylate rRNA and affect RNA processing[5]; the only other known glutamine methyltransferases in yeast (Mtq1 and Mtq2) modify translational release factors on a conserved glutamine[3]. Thus, glutamine methylation may have evolved to be a modification dedicated to a specific cellular process. Finally, our finding that a protein can catalyse the methylation of proteins and RNA, opens the possibility that many other enzymes may have such dual specificity.

Online Only Methods

Strains, plasmids and reagents

Genotypes of strains and yeast plasmids used in this work are listed in Supplementary Table 1. If not stated otherwise, all strains used are derivatives of W303. Integrations and deletions were performed using one-step PCR-based methods[31,32]. All plasmids used were verified by sequencing. Non-radioactive S-Adenosylmethionine (SAM) and recombinant histones were purchased from New England Biolabs (NEB) and tritiated SAM from Perkin Elmer. Peptides for immunisation were from ChemPep Inc. and biotinylated peptides were from Cambridge Peptides using Fmoc-Gln(Me)-OH (ChemPep Inc). Ni-NTA and IgG Sepharose were from GE Healthcare, Amylose resin from NEB and Streptactin-Sepharose from iBA. Streptavidine, Protein A and Protein G Dynabeads were from Invitrogen. (D)-Desthiobiotin was purchased from Sigma and Factor Xa from NEB. FlexiTube siRNA was from Qiagen (FBL_5: 5′-ACACTTTGTGATTTCCATTAA-3′ and FBL_6: 5′-ATCGTTGGTCCGGATGGTCTA-3′) and siRNA transfection reagent Ribocellin was from BCC. Protease Inhibitors were from Roche. DMEM-H/F12, penicillin-streptomycin-fungizome and epidermal growth factor were from Invitrogen, cholera toxin from List Biological Laboratories, Inc. Insulin and Hydrocortisone were from Sigma. MTT assays were purchased from Invitrogen. Alpha factor was from GenScript and Pronase from Calbiochem.

Antibodies

The Q105me antibody was produced using the Eurogentec Speedy 28-day polyclonal package. Sera were purified using unmodified and modified peptide columns and tested for specificity (Extended Data Fig. 3). Anti-H2A (ab13923 – for Fig. 1c) mouse anti-fibrillarin (ab4566 - for immunofluorescence), rabbit anti-fibrillarin (ab5821 – for western blot) and mouse anti-HA (ab1424) were from Abcam. Anti-myc (9E10 – for ChIP), rabbit anti-c-myc (C3956 – for western blot), anti-biotin (B7653) and anti-FLAG (M2) were from Sigma, anti-γH2A (39235) and anti-H3K56Ac (61061) were from Active Motif. Anti-CBP tag (K-24), anti-SSRP1 (D-7) and anti-Spt16 (H-4) were from Santa Cruz. All antibodies were used as suggested by the supplier; anti-H2AQ105me was diluted 1/10000 for western blotting, 1/50 for ChIPs and 1/100 for immunofluorescence.

Protein Purification

Proteins were expressed in BL21 Codon Plus. For FACT, Spt16 and Pob3 were cloned into the pDuet series of Novagen. Cells were grown in LB to an OD_{600} of 1 at 37°C. Cells were then shifted to 20°C for one hour before induction with 1mM IPTG over night. Cells were lysed in buffer A (20mM HEPES•KOH pH7.5, 50mM KCl, 20mM Imidazol, 5mM β-Mercaptoethanol, 10% glycerol) supplemented with 1mg/ml lysozyme. Cells were lysed using 6 × 30″ pulses on a Branson Sonifier. The lysate was centrifuged and supernatant was bound to 1ml Ni-NTA for 2h at 4°C. The matrix was washed with 100 ml buffer A and eluted in the same buffer supplemented with 250 mM Imidazole. The eluate was bound to 2 ml Streptactin-Sepharose for 2 h at 4°C. Subsequently, the matrix was washed using 100 ml buffer A and Spt16/Pob3 were eluted in the same buffer containing 2.5 mM D-Desthiobiotin.

Nop1 was expressed in BL21 Codon Plus as a Maltose-Binding-Protein fusion and purified using the pMal System (NEB) according to the manufacturers protocol. Nop1 was eluted off the matrix by Factor Xa cleavage. The protein was polished over a Recource S column and a linear gradient from 150 – 500 mM NaCl.

H2A and derivatives were purified as described[3].

Activity Assays

For peptide-based activity assays, peptides (5mg/ml) were bound to Streptavidine-coated M280 beads (20 μl of slurry and 1.6μl peptide /reaction) and incubated for 1h at room temperature in TBS/0.1% NP40. Beads were washed several times to remove unbound peptide. For the reaction, the equivalent of 20 μl beads were distributed into microtubes. 50 μl extract (see below) and 1 μl [3H]-SAM were added. Incubate at 30°C for 30 min. Subsequently, 1 μl of [3H]-SAM was added and the reaction was incubated for another 30 min. Beads were washed 3x with 200 μl TBS/0.1% NP40 and once in 200 μl TBS/ 1M NaCl/ 0.1%NP40. Beads were resuspended in 200 μl TBS/0.1% NP40 and boiled for 5 min. 100 μl of supernatant were counted in a scintillation counter.

For assays on recombinant H2A, 0.2 μg of Nop1 was assayed on 1 μg of recombinant H2A in the presence of 100 μM SAM in ½ TBS and 1mM DTT for 30 min at 30°C. Half of the reaction was loaded on a SDS-PAGE for Coomassie staining and 2% of the reaction for western blotting.

Extract preparation for activity assays and Mass Spectrometry

3l of yeast were grown to OD_{600} ~ 0.6. The cell pellet was washed twice with ice-cold PBS. The pellet was resuspended in 2x volume of Nuclear Lysis buffer (10mM Tris pH8, 420mM NaCl, 2mM EDTA, 10% glycerol, 0.1% NP40, 1mM DTT) supplemented with protease inhibitors. Small droplets were made into liquid nitrogen. Cells were lysed by grinding on liquid nitrogen in a mortar for 10-15 minutes. The powder was thawed quickly at 30°C and put back on ice for 10min. The cell lysate was centrifuged for 2 min at 4000rpm in tabletop centrifuge at 4°C to remove unbroken cells. This crude lysate was extracted for another 30 min on ice before centrifuging it for 10 min 13k rpm at 4°C. The Supernatant was diluted into 10mM Tris, 5mM MgCl2, 10% glycerol, 1mM DTT and bound to a 1ml equilibrated DEAE column. The column was washed with 10 column volume (CV) and proteins were step eluted with 150mM, 300mM, 500mM, 1000mM NaCl (500μl fractions). The fractions were dialysed over night into in 10mM Tris, 150mM NaCl, 5mM MgCl2, 10% glycerol, 1mM DTT and used for activity assays. The fraction containing the activity was run on a SDS-PAGE and processed for LC-MS/MS analysis at the Cambridge Centre for Proteomics, Department of Biochemistry, University of Cambridge. Protein hits were identified using Mascot Software.

Extracts for TAP-tag purification were generated as described above. The cleared lysate was then incubated with 200 μl IgG Sepharose beads for 2h at 4°C and treated as described for the original TAP-tag protocol. Briefly, the beads were washed with 30 ml of IPP150 and 10 ml of TEV-cleavage buffer, followed by TEV cleavage at 4°C over night.

Peptide Pulldowns

For peptide IPs, 15 μl of the respective peptides (at 5 mg/ml) were diluted in 200ul TBS/ 0.1% NP40 and incubate with an equivalent of 100 μl of equilibrated slurry for 1h at room temperature. Beads were washed 2x with 1 ml TBS/0.1% NP40 and washed beads were incubated with 1ug of Spt16/Pob3 (10nM final) in 500 μl TBS/0.1% NP40, 1mM DTT for 2h at 4°C. Subsequently, beads were washed 4x 1 ml with TBS/0.1% NP40 1mM DTT and eluted with 50 μl SDS-sample buffer.

Phage Display Assay

We used the Ph.D.™-12 Phage Display Peptide Library Kit from New England Biolabs to screen for a potential Spt16/Pob3 interaction site within H2A using the manufacturers instruction. As a bait we used His6-tagged Spt16/StrepII-Pob3. In the first selection round we used Ni-NTA, in the second Streptactin and in the third round we used both matrices for

affinity purification. DNA of enriched phages was prepped and sequenced using the kit's primer.

Chromatin Immunoprecipitation - ChIP

Chromatin was sonicated to produce fragments of 400-500 bp. Chromatin inmunoprecipitation was performed essentially as described[30], except ChIPs for H2AQ105me, in which case 5 times more chromatin was used as input. Real time PCR analysis was performed on a StepOnePlus system using Fast SYBR Green (Applied Biosystems). Standard curves for each primer set were calculated from amplification of diluted DNA. After each run, a dissociation curve was performed to ensure that no primer dimers contaminated the quantification and that the product had the expected melting temperature. Each PCR reaction was performed in duplicate and the signal intensity value for each sample was calculated from the average of the 2 experiments. Primer sequences are shown in Supplementary Table 2. Relative fluorescent intensities for the ChIP experiments were calculated as follows: (Ab signal-IgG signal) /(input signal - IgG signal), where Ab is the antibody of interest, IgG is the negative control antibody and input the sheared genomic DNA. Each experiment was repeated between 2 and 4 times from independent cultures.

ChIP-Seq

50% of a ChIP reaction was used to generate the library. Library production followed the protocol published on http://ethanomics.wordpress.com/chip-seq-library-construction-using-the-illumina-truseq-adapters/ (2012) with few changes. Purifications steps using AMPure XP bead were replaced by the ChIP DNA Clean & Concentrator kit by Zymoresearch. Illumina adaptors were exchanged for Bioo Nextflex adaptors 1-3 (1:100 dilution each). Size selection was performed on a SAGE Pippin Prep using 2% gels and selecting for a size between 350-600 bp. The quality of the library was assessed using Agilent DNA High Sensitivity ChIPs and Qiagen Qubit. Libraries were pooled and sequenced on a Illumina MiSeq using single-ended 50bp reads

Transcriptional Run-On

Nuclear Run-On was performed essentially as described earlier[33]. Briefly, cells were inoculated to a starting A_{600} of ~0.03 and grown in YPAD medium to an A_{600} of ~0.1 to 0.15. 5 A_{600} units of culture (~5×10^7 cells) were harvested by centrifugation at 3,000 × *g* for 3 min. Cells were resuspended in 5 ml of ice-cold H_2O and then centrifuged at 4°C for 3 min at 3,000 × *g*. The cells were then resuspended in 950 μl of ice-cold H_2O, and 50 μl of 10% Sarkosyl was added. The sample was gently mixed and incubated on ice for 20 min. The permeabilized cells were pelleted by microcentrifugation for 1 min, and the supernatant was carefully removed. Residual supernatant was removed after a second brief microcentrifugation.

The cells were suspended in 97.5 μl of transcription buffer (50 mM Tris hydrochloride (pH 8), 100 mM KCI, 5 mM MgCl2, 1 mM MnCl2, 2 mM DTT) supplemented with 40U of RNase OUT (Invitrogen). Reactions were started by addition of 2.5 μl of RNA biotin labeling mix (Roche) and shift to 30°C. After 5 minutes the reaction was pipetted into a fresh eppendorf tube with 250 μl glass beads and 1ml Trizol reagent (Invitrogen) on ice. Cells were lysed and homogenized by bead beating for 4x 1 minute with 3 minutens incubation on ice in between. After the last vortexing, the reactions were incubated at room temperature for 5 minutes followed by RNA extraction following the Trizol. The RNA pellet was resuspended in 200μl of 10 mM Tris-HCl (pH 7.5), 1 mM EDTA, 100 mM NaCl and 50 μl of washed T1-streptacidine dynabeads were added for 2h at RT. Beads were washed twice in 500 μl of 2× SSC (1× SSC is 0.15 M NaCl plus 0.015 M sodium citrate), 15% formamide for 15 min and once in 500 μl of 2× SSC for 5 min. Beads were

Europe PMC Funders Author Manuscripts

resuspended in 12 μl RNase free water and RNA was reverse transcribed. Sequences of primers used for qPCR are given in Supplementary Table 2.

Sequence Mapping

Called reads from the Illumina MiSeq system were mapped to the latest version of the *Saccharomyces cerevisiae* genome (sacCer3) using the Burrows Wheeler Aligner (BWA) with parameters −n 10 −k 3 −l 20[34]. PCR duplicates mapping to identical regions on the genome were removed using SamTools[35]. Filtered mapped reads were extended to the fragment length of 400 bp and converted to wiggle format using the bedTools suite of utilities[36]. Raw and mapped reads are given in Supplementary Table 3.

Normalisation

Extended reads were counted in bins of 50 bp across the entire genome and were normalised to the total number of mapped reads for each sample to account for differences in read depth. Within each bin, the level of Q105me enrichment above H2A control was determined by first subtracting the IgG read count and subsequently thresholding at a minimum value of one (adjusted value). The normalised Q105me count was generated by dividing the adjusted Q105me values by the adjusted H2A count. Data were transformed to a log2 scale for visualisation.

Western Blot

Western blot of total yeasts extracts were performed by standard procedures. Transfer to nitrocellulose membranes were made on carbonate buffer (21.1g/L NaHCO3, 18.35g/L Na2CO3, pH: 9.5) at 45mA for 70 min. The membranes were blocked for 1 h at room temperature in TBS+ 0.1% Tween-20+ 5% BSA; primary antibody was incubated at 4°C over night and secondary for 1h at room temperature.

Cell Culture

MCF 10A (CRL-10317) cells were obtained from American Type Culture Collection (Rockville, MD) and were grown in DMEM-H/F12 medium supplemented with 1% penicillin-streptomycin-fungizome, 10 μg/ml insulin, 100 ng/ml cholera toxin, 20 ng/ml epidermal growth factor, 500 ng/ml hydrocortisone and 5% FBS at 37 °C in 5% CO_2 humidified atmosphere. NIH-3t3 were grown in DMEM supplemented with PenStrep and 5% FBS at 37 °C in 5% CO_2 humidified atmosphere.

Transfections of siRNA were carried out according to manufacturers instructions. For 10cm dishes, 750000 cells were seeded and transfected 24h later. For any other dish, cell numbers were adjusted to area. MTT assays were performed according to the manufacturers protocol.

Immunofluorescence

Cells were processed for immunofluorescence as described earlier[37], but primary antibody incubation was over night at 4°C. Images were acquired using a Olympus FV1000 upright system equipped with a 60x/1.35 UPlanSApo Oil and a 100x/1.40 UPlanSApo Oil objective. Images were processed further using the ImageJ software package.

In-gel digestion

Proteins were resolved on 4-20% SDS-PAGE. The gel was stained with colloidal Coomassie blue, cut into 20 slices and processed for mass spectrometric analysis as previously described[38]. Briefly, cysteines were reduced with dithiothreitol (DTT), alkylated using chloroacetamide[39] (CAA), digested overnight with trypsin and loaded onto StageTips prior to mass spectrometric analysis[40].

Mass spectrometric analysis

All MS experiments were performed on a nanoscale HPLC system (EASY-nLC from Thermo Fisher Scientific) connected to a hybrid LTQ–Orbitrap XL (Thermo Fisher Scientific) equipped with a nanoelectrospray source. Each peptide sample was separated on a 15 cm analytical column (75 m inner diameter) packed in-house with 3 micrometer C18 beads (Reprosil Pur-AQ, Dr. Maisch) with a 2h gradient from 5% to 40% acetonitrile in 0.5% acetic acid. The eluate from the HPLC was directly electrosprayed into the mass spectrometer. The MS instrument was operated in data-dependent mode to automatically switch between full-scan MS and MS/MS acquisition. Survey full-scan MS spectra (from m/z 300–1,800) were acquired in the Orbitrap analyzer with resolution R = 60,000 at m/z 400 after accumulation to a 'target value' of 1,000,000 in the linear ion trap using 'Top10' method. The ten most intense peptide ions with charge states ≥ 2 were sequentially isolated to a target value of 3,000 using automatic gain control (AGC) and fragmented by collisional induced dissociation (CID) in the linear quadrupole ion trap (LTQ).

Identification of peptides and proteins by MaxQuant

The data analysis was performed with the MaxQuant software (version 1.2.7.1, www.maxquant.org) as described[41] supported by Andromeda as the database search engine for peptide identifications[42]. MS/MS peak lists were generated by filtering spectra to contain at most six peaks per 100 Th interval and subsequently searched by Andromeda against a concatenated target/decoy (forward and reversed) version of the Uniprot human database (68,079 forward protein entries). Protein sequences of common contaminants such as human keratins and proteases used were added to the database. The initial mass tolerance in MS mode was set to 7 p.p.m. and MS/MS mass tolerance was 0.5 Th. Cysteine carbamidomethylation was set as a fixed modification, whereas protein N-acetylation, and oxidized methionine were set as variable modifications. A maximum of two missed cleavages were allowed while we required strict tryptic specificity. All top-scoring peptide assignments made by Andromeda were filtered based on previous knowledge of individual peptide mass error. Peptide assignments were statistically evaluated in a Bayesian model on the basis of sequence length and Andromeda score as described[43]. Only peptides and proteins with a false discovery rate of less than 1% were accepted, estimated on the basis of the number of accepted reverse hits.

Statistics

Average (mean), sem. were calculated in Prism (Graphpad) and statistical significance based on Student's *t*-test (always two-tailed) in Excel. All experiments were performed at least in triplicates (biological replicates). * indicates a p-value $p<0.05$ and ** $p<0.01$.

Supplementary Material

Refer to Web version on PubMed Central for supplementary material.

Acknowledgments

We would like to thank Ed Hurt, David Stillman, Takehiko Kobayashi, Jeffrey Smith and Jef Boeke for providing strains; Kathryn Lilley for Mass spectrometry and Michiel Vermeulen for help with the identification of H2AQ104me; Sylviane Moss for running of the Illumina MiSeq; members of the Kouzarides lab for discussions; and Andy Bannister and Rimma Belotserkovskaya for critical reading of the manuscript. This work has been funded by a programme grant from Cancer Research UK and a project grant from the BBSRC (BB/K017438/1).

References

1. Kouzarides T. Chromatin modifications and their function. Cell. 2007; 128:693–705. [PubMed: 17320507]
2. Formosa T. The role of FACT in making and breaking nucleosomes. Biochim Biophys Acta. 2012; 1819:247–255. [PubMed: 21807128]
3. Polevoda B, Sherman F. Methylation of proteins involved in translation. Molecular Microbiology. 2007; 65:590–606. [PubMed: 17610498]
4. Petrossian TC, Clarke SG. Multiple Motif Scanning to identify methyltransferases from the yeast proteome. Molecular & Cellular Proteomics. 2009; 8:1516–1526. [PubMed: 19351663]
5. Tollervey D, Lehtonen H, Jansen R, Kern H, Hurt EC. Temperature-sensitive mutations demonstrate roles for yeast fibrillarin in pre-rRNA processing, pre-rRNA methylation, and ribosome assembly. Cell. 1993; 72:443–457. [PubMed: 8431947]
6. Gautier T, Bergès T, Tollervey D, Hurt E. Nucleolar KKE/D repeat proteins Nop56p and Nop58p interact with Nop1p and are required for ribosome biogenesis. Molecular and Cellular Biology. 1997; 17:7088–7098. [PubMed: 9372940]
7. Fath S, et al. Association of yeast RNA polymerase I with a nucleolar substructure active in rRNA synthesis and processing. The Journal of Cell Biology. 2000; 149:575–590. [PubMed: 10791972]
8. Krogan NJ, et al. Global landscape of protein complexes in the yeast Saccharomyces cerevisiae. Nature. 2006; 440:637–643. [PubMed: 16554755]
9. Lambert J-P, Mitchell L, Rudner A, Baetz K, Figeys D. A novel proteomics approach for the discovery of chromatin-associated protein networks. Molecular & Cellular Proteomics. 2009; 8:870–882. [PubMed: 19106085]
10. Jansen RP, et al. Evolutionary conservation of the human nucleolar protein fibrillarin and its functional expression in yeast. The Journal of Cell Biology. 1991; 113:715–729. [PubMed: 2026646]
11. Amin MA, et al. Fibrillarin, a nucleolar protein, is required for normal nuclear morphology and cellular growth in HeLa cells. Biochem Biophys Res Commun. 2007; 360:320–326. [PubMed: 17603021]
12. Raška I, Shaw PJ, Cmarko D. Structure and function of the nucleolus in the spotlight. Curr Opin Cell Biol. 2006; 18:325–334. [PubMed: 16687244]
13. Albert B, Perez-Fernandez J, Léger-Silvestre I, Gadal O. Regulation of ribosomal RNA production by RNA polymerase I: does elongation come first? Genet Res Int. 2012; 2012:276948. [PubMed: 22567380]
14. Grummt I, Längst G. Epigenetic control of RNA polymerase I transcription in mammalian cells. Biochim Biophys Acta. 2012 doi:10.1016/j.bbagrm.2012.10.004.
15. Ide S, Miyazaki T, Maki H, Kobayashi T. Abundance of ribosomal RNA gene copies maintains genome integrity. Science. 2010; 327:693–696. [PubMed: 20133573]
16. Gorenstein C, Atkinson KD, Falkes EV. Isolation and characterization of an actinomycin D-sensitive mutant of Saccharomyces cerevisiae. J. Bacteriol. 1978; 136:142–147. [PubMed: 361685]
17. VanDemark AP, et al. Structural and functional analysis of the Spt16p N-terminal domain reveals overlapping roles of yFACT subunits. J Biol Chem. 2008; 283:5058–5068. [PubMed: 18089575]
18. McCullough L, et al. Insight into the mechanism of nucleosome reorganization from histone mutants that suppress defects in the FACT histone chaperone. Genetics. 2011; 188:835–846. [PubMed: 21625001]
19. Smith JS, Boeke JD. An unusual form of transcriptional silencing in yeast ribosomal DNA. Genes & Development. 1997; 11:241–254. [PubMed: 9009206]
20. Johnson JM, et al. Rpd3 and Spt16-mediated nucleosome assembly and transcriptional regulation on yeast rDNA genes. Molecular and Cellular Biology. 2013 doi:10.1128/MCB.00112-13.
21. Hainer SJ, Pruneski JA, Mitchell RD, Monteverde RM, Martens JA. Intergenic transcription causes repression by directing nucleosome assembly. Genes & Development. 2011; 25:29–40. [PubMed: 21156811]

22. Orphanides G, Wu WH, Lane WS, Hampsey M, Reinberg D. The chromatin-specific transcription elongation factor FACT comprises human SPT16 and SSRP1 proteins. Nature. 1999; 400:284–288. [PubMed: 10421373]
23. Birch JL, et al. FACT facilitates chromatin transcription by RNA polymerases I and III. EMBO J. 2009; 28:854–865. [PubMed: 19214185]
24. Belotserkovskaya R, et al. FACT facilitates transcription-dependent nucleosome alteration. Science. 2003; 301:1090–1093. [PubMed: 12934006]
25. Winkler DD, Muthurajan UM, Hieb AR, Luger K. Histone Chaperone FACT Coordinates Nucleosome Interaction through Multiple Synergistic Binding Events. Journal of Biological Chemistry. 2011; 286:41883–41892. [PubMed: 21969370]
26. Formosa T, et al. Defects in SPT16 or POB3 (yFACT) in Saccharomyces cerevisiae cause dependence on the Hir/Hpc pathway: polymerase passage may degrade chromatin structure. Genetics. 2002; 162:1557–1571. [PubMed: 12524332]
27. Wittner M, et al. Establishment and Maintenance of Alternative Chromatin States at a Multicopy Gene Locus. Cell. 2011; 145:543–554. [PubMed: 21565613]
28. Choudhary C, et al. Lysine acetylation targets protein complexes and co-regulates major cellular functions. Science. 2009; 325:834–840. [PubMed: 19608861]
29. Wang B, Malik R, Nigg EA, Körner R. Evaluation of the low-specificity protease elastase for large-scale phosphoproteome analysis. Anal Chem. 2008; 80:9526–9533. [PubMed: 19007248]
30. Santos-Rosa H, et al. Methylation of histone H3 K4 mediates association of the Isw1p ATPase with chromatin. Molecular Cell. 2003; 12:1325–1332. [PubMed: 14636589]
31. Janke C, et al. A versatile toolbox for PCR-based tagging of yeast genes: new fluorescent proteins, more markers and promoter substitution cassettes. Yeast. 2004; 21:947–962. [PubMed: 15334558]
32. Longtine MS, et al. Additional modules for versatile and economical PCR-based gene deletion and modification in Saccharomyces cerevisiae. Yeast. 1998; 14:953–961. [PubMed: 9717241]
33. Patrone G, et al. Nuclear run-on assay using biotin labeling, magnetic bead capture and analysis by fluorescence-based RT-PCR. BioTechniques. 2000; 29:1012–4. 1016–7. [PubMed: 11084863]
34. Li H, Durbin R. Fast and accurate short read alignment with Burrows-Wheeler transform. Bioinformatics. 2009; 25:1754–1760. [PubMed: 19451168]
35. Li H, et al. The Sequence Alignment/Map format and SAMtools. Bioinformatics. 2009; 25:2078–2079. [PubMed: 19505943]
36. Quinlan AR, Hall IM. BEDTools: a flexible suite of utilities for comparing genomic features. Bioinformatics. 2010; 26:841–842. [PubMed: 20110278]
37. Bartke T, et al. Nucleosome-interacting proteins regulated by DNA and histone methylation. Cell. 2010; 143:470–484. [PubMed: 21029866]
38. Shevchenko A, Wilm M, Vorm O, Mann M. Mass spectrometric sequencing of proteins silver-stained polyacrylamide gels. Anal Chem. 1996; 68:850–858. [PubMed: 8779443]
39. Nielsen ML, et al. Iodoacetamide-induced artifact mimics ubiquitination in mass spectrometry. Nat Meth. 2008; 5:459–460.
40. Rappsilber J, Ishihama Y, Mann M. Stop and go extraction tips for matrix-assisted laser desorption/ionization, nanoelectrospray, and LC/MS sample pretreatment in proteomics. Anal Chem. 2003; 75:663–670. [PubMed: 12585499]
41. Cox J, Mann M. MaxQuant enables high peptide identification rates, individualized p.p.b.-range mass accuracies and proteome-wide protein quantification. Nature Biotechnology. 2008; 26:1367–1372.
42. Cox J, et al. Andromeda: a peptide search engine integrated into the MaxQuant environment. J. Proteome Res. 2011; 10:1794–1805. [PubMed: 21254760]
43. Cox J, et al. A practical guide to the MaxQuant computational platform for SILAC-based quantitative proteomics. Nat Protoc. 2009; 4:698–705. [PubMed: 19373234]

Europe PMC Funders Author Manuscripts

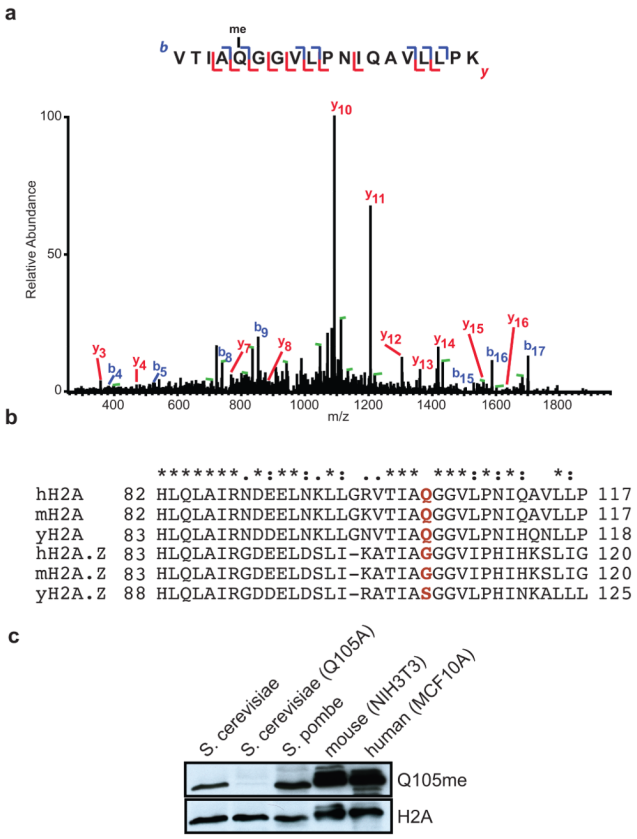

Figure 1. Identification and localisation of methylated H2A glutamine 105

a) Tandem mass spectrum (MS/MS) of the Q104me modified peptide VTIAQGGVLPNIQAVLLPK from H2A. The y and b series indicate fragments at amide bonds of the peptide, unambiguously identifying the methylated glutamine 104 (mammalian cells – yeast: glutamine 105). b) Alignment of the region encompassing Q105 of H2A and its variant H2A.Z. Highlighted in red is Q105 in H2A and the corresponding change to glycine or serine in H2A.Z. c) Analysis of yeast and mammalian cell extracts for the presence of Q105 methylation using a modification specific antibody.

Europe PMC Funders Author Manuscripts

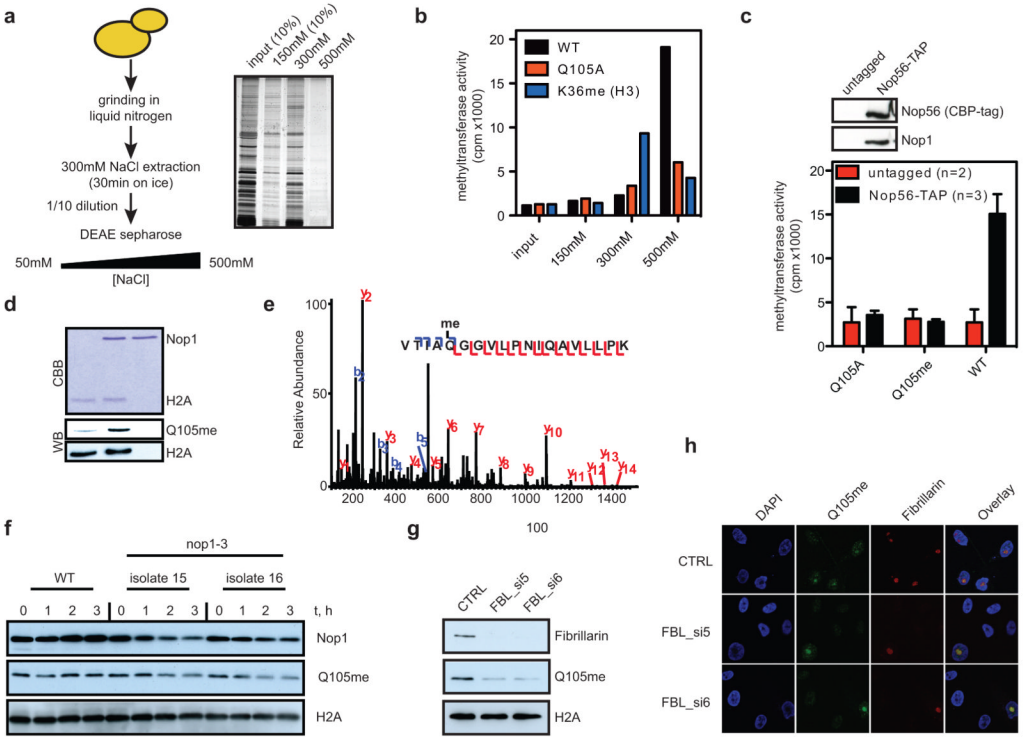

Figure 2. Identification of Nop1/Fibrillarin as the methyltransferase of Q105

a) General strategy. b) Fractions from (a) were assayed on peptides containing glutamine or alanine at position 105 and compared to an unrelated peptide (H3K36me). For this, peptides were bound to Dynabeads, incubated with extract and [^{3}H]-SAM and after extensive washes, analysed by liquid scintillation. Representative data of three independent experiments is shown. c) TAP-tag purification of the Nop1 complex coupled to the same activity assay as in (b) recapitulates the activity as found in the DEAE fraction. d) Recombinant Nop1 was incubated with SAM and recombinant histone H2A. Coomassie stain (CBB) and western blot (WB) of the reaction are shown. e) Tandem mass spectrum (MS/MS) of the Q104me modified peptide from H2A, which unambiguously identifies the methylated glutamine 104. f) Strains carrying thermosensitive alleles (15 and 16) of Nop1 were analysed for loss of Q105 methylation levels upon shift to restrictive temperature. g) The mammalian homolog of Nop1, Fibrillarin was knocked-down by independent siRNAs and probed for loss of Q105 methylation 48 h after transfection. A scrambled siRNA served as control (CTRL). h) Immunofluorescence of cells treated as in g) were stained using the Q105me-specific and anti-Fibrillarin antibodies and counterstained with DAPI as nuclear marker.

Europe PMC Funders Author Manuscripts

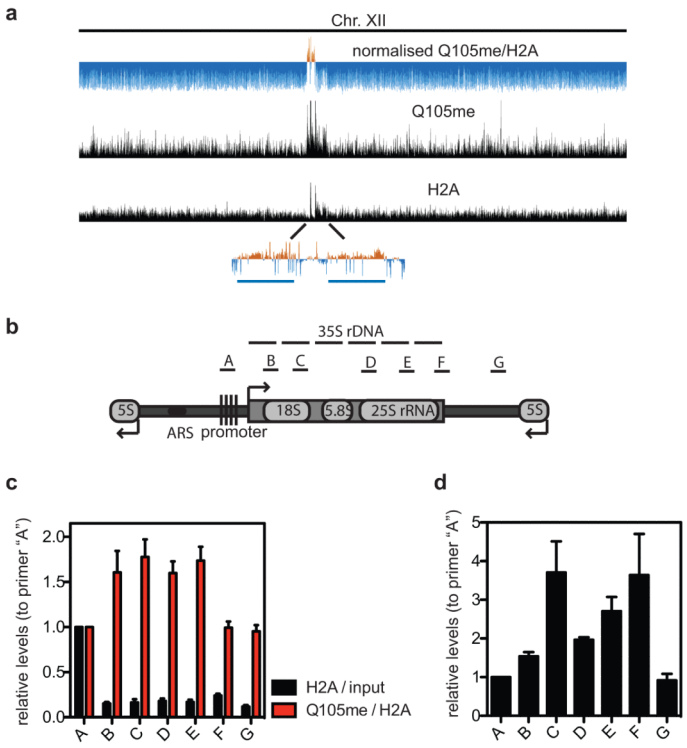

Figure 3. Genomic landscape of Q105me

a) ChIP-Seq profile of Q105me and H2A over Chromosome 12. The upper plot represents the normalised tracks for the mapped reads of Q105me/H2A. The magnification of the enriched region shows the rDNA region located on this chromosome. The two blue bars represent the 35S transcripts that are present in the genome annotation. b) Schematic representation of one rDNA repeat with the position of primers used to scan the rDNA region by ChIP qPCR. c) ChIP-qPCR validation of the ChIP-Seq shown in (a). d) Nop1 profile over the rDNA locus. The ChIP-qPCR profile was internally normalised to signal of primer pair "A". ChiP-qPCR data shows the mean ± SEM of three independent biological experiments.

Europe PMC Funders Author Manuscripts

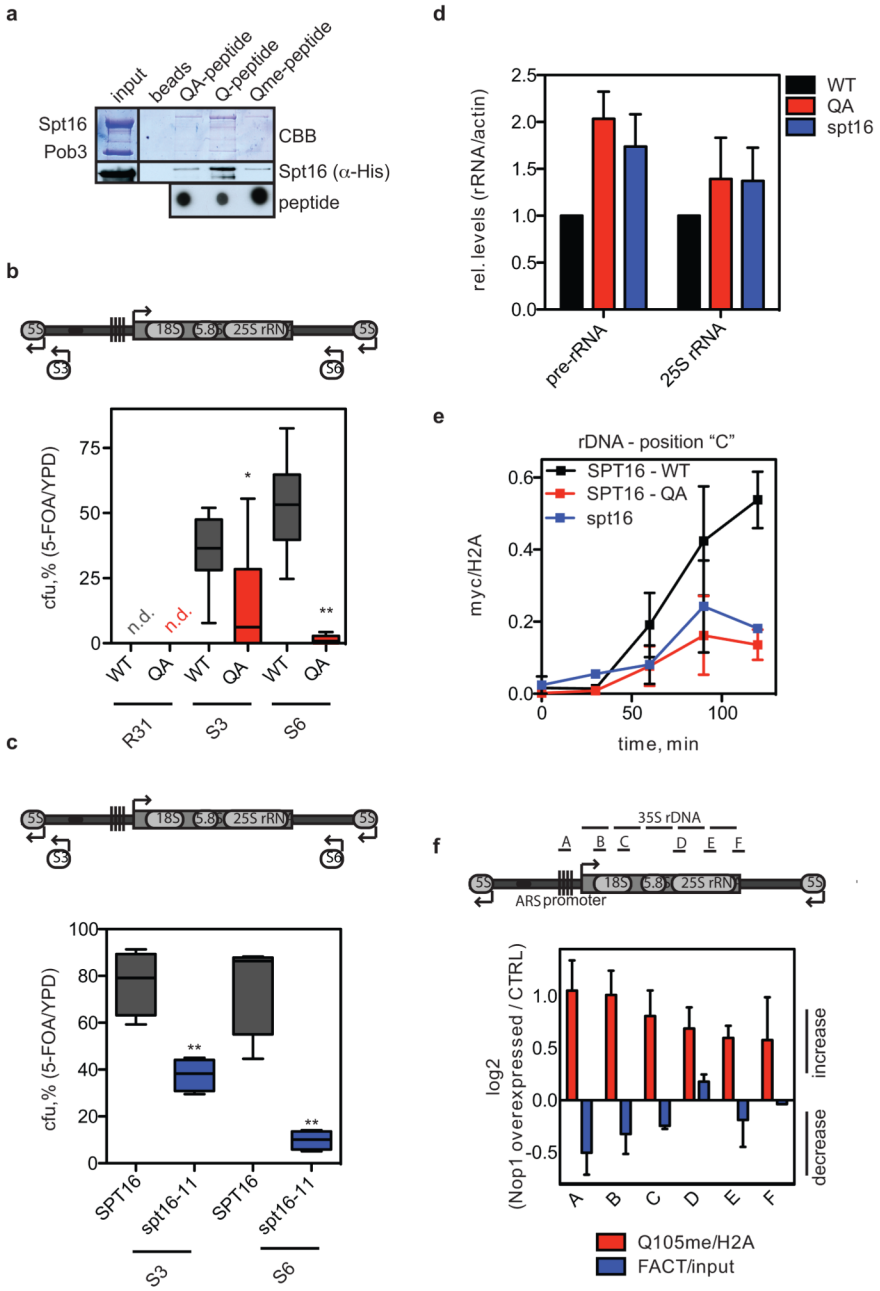

Figure 4. Unmodified Q105 is part of a recognition motif for FACT

a) Indicated peptides were bound to Streptavidine-Dynabeads and incubated with recombinantly purified Spt16/Pob3 for 4h at 4°C. Input represents 50% of Spt16/Pob3 used for the IP. Bound Spt16/Pob3 was analysed by Coommassie stain (CBB) or western blotting. Peptides were spotted on membrane as loading control. b) Effect of the H2AQ105A mutant on the transcription of a *URA3* reporter integrated at the indicated positions in the rDNA repeat (S3 and S6) and R31 outside the rDNA[19]. Strains were assayed for their ability to grow on 5-FOA for three days at 30°C (n≥3, n.d. – not detected) c) The *spt16-11* allele was assayed as described in c), but colonies were counted after one week. d) Yeast expressing either wild-type (WT) or Q105A (QA) mutant H2A as sole source of histones were assayed for rDNA transcription by transcriptional run-on and compared to cells that carry an *spt16*

Europe PMC Funders Author Manuscripts

thermosensitive allele (*spt16*). RNA levels are expressed as relative levels to actin (* represents $p<0.05$ and ** $p<0.01$). e) Differences in histone incorporation rates between WT and Q105A (QA) histones. WT H2A and H2AQ105 were myc-tagged and placed under the control of a galactose inducible promoter in either wild-type or *spt16-11* cells. Myc-tagged histones were induced by addition of 2% galactose (t=0). Samples were taken at the indicated time points and chromatin immunoprecipitated with anti-myc and H2A antibodies. f) Nop1 over-expression (Nop1 overexpressed) leads to an increase of Q105 methylation and a concurrent decrease in FACT occupancy at the rDNA locus. Primer positions are indicated and data was presented as the log2 changes compared to an empty vector control (CTRL). ChiP-qPCR data shows the mean ± SEM of at least two independent biological experiments.